

Prediction of anomalous LA-TA splitting in electrifieds

Cite as: Matter Radiat. Extremes 6, 038403 (2021); doi: 10.1063/5.0043276

Submitted: 7 January 2021 • Accepted: 24 March 2021 •

Published Online: 16 April 2021



View Online



Export Citation



CrossMark

Leilei Zhang,  Hua Y. Geng, ^{a)} and Q. Wu

AFFILIATIONS

National Key Laboratory of Shock Wave and Detonation Physics, Institute of Fluid Physics, CAEP, P.O. Box 919-102, Mianyang, Sichuan 621900, People's Republic of China

^{a)} Author to whom correspondence should be addressed: s102genghy@caep.cn

ABSTRACT

Electrifieds are an emerging class of materials with excess electrons localized in interstices and acting as anionic interstitial quasi-atoms (ISQs). The spatial ion–electron separation means that electrifieds can be treated physically as ionic crystals, and this unusual behavior leads to extraordinary physical and chemical phenomena. Here, a completely different effect in electrifieds is predicted. By recognizing the long-range Coulomb interactions between matrix atoms and ISQs that are unique in electrifieds, a nonanalytic correction to the forces exerted on the matrix atoms is proposed. This correction gives rise to a longitudinal acoustic–transverse acoustic splitting in the acoustic branch of lattice phonons near the zone center, similar to the well-known longitudinal optical–transverse optical splitting in the phonon spectra of ionic compounds. The factors that govern this splitting are investigated, with isotropic fcc-Li and anisotropic hP4-Na as the typical examples. It is found that not all electrifieds can induce a detectable splitting, and criteria are given for this type of splitting. The present prediction unveils the rich phenomena in electrifieds and could lead to unprecedented applications.

© 2021 Author(s). All article content, except where otherwise noted, is licensed under a Creative Commons Attribution (CC BY) license (<http://creativecommons.org/licenses/by/4.0/>). <https://doi.org/10.1063/5.0043276>

I. INTRODUCTION

The phonon dispersion relation $\omega(\mathbf{q})$ of a crystalline lattice reflects the energy variation in the quantum vibrations of a solid. This quantity encodes all information about the ionic contributions to the thermodynamic properties and dynamic process at low temperature, which is fundamental for both equilibrium and nonequilibrium statistics of a solid. Normally, there are three acoustic branches and $3N-3$ optical branches for a three-dimensional crystal comprising N ($N \rightarrow \infty$) atoms, and their frequencies are denoted as ω_A and ω_O , respectively. For nonpolar crystals, the long-wavelength longitudinal optical (LO) and transverse optical (TO) modes could be degenerate near the zone center (ZC). However, in ionic crystals, the relative vibrations of positively and negatively charged ions induce a macroscopic electric field (E-field), which in turn affects the motion of ions.^{1,2} This long-range Coulomb interaction (LRCI) lifts the aforementioned degeneracy and gives rise to LO-TO splitting near the Brillouin ZC ($\omega_{LO} \neq \omega_{TO}$, $q \approx 0$), which is very important for describing accurately the dielectric properties and phonon transportation in a polar system and has been widely explored.^{3–8}

Electrifieds^{9–20} are an emerging class of materials in which highly localized excess electrons locate at lattice interstitial sites and behave

as anionic interstitial quasi-atoms (ISQs).^{11,21–24} Electrifieds have promising physical and chemical properties due to the unique electronic structures that originate from the localized ISQs. For example, they open the energy gap and lead to counterintuitive metal–nonmetal transitions in Li^{25,26} and Na,²⁷ as well as an accompanying complex structural phase transition in dense Li.²⁶ This extraordinary behavior of the localized electrons not only modifies the electronic and crystalline structure greatly but also changes the dielectric and optical properties,²⁸ thereby making semi-transparent metals possible.²⁸

Physically, electrifieds are analogous to ionic compounds and are intrinsically polar. The difference is that the negatively charged ISQs take the role of anions in electrifieds. Therefore, the vibrations of positively charged matrix atoms in an electrified will induce a non-negligible macroscopic E-field that leads to LRCI and a nonanalytical contribution to the dielectric terms near the ZC. Herein, we propose a theoretical model to describe this nonanalytical contribution. The resultant effect in the phonon dispersion is explored, which gives an anomalous splitting in the long-wavelength longitudinal acoustic (LA) and transverse acoustic (TA) branches near the ZC. This novel but counterintuitive LA-TA splitting in electrifieds is a direct

counterpart of the well-known LO-TO splitting in classical polar systems and demonstrates the direct physical consequence of the strong long-range coupling of localized electrons and crystalline matrix atoms. It also acts as a typical example that reveals the direct participation of electrons in sound propagation in condensed matter.

The methodology and computational details are presented in Sec. II, the results and analysis are given in Sec. III, and criteria (or rules of thumb) for this extraordinary LA-TA splitting to occur are summarized in Sec. IV, together with relevant discussions. Finally, the conclusion and summary of main findings are given in Sec. V.

II. METHODOLOGY AND COMPUTATIONAL DETAILS

A. Basic theory

In the quantum mechanics of solids, the electronic and nuclear subsystems can be decoupled using the Born–Oppenheimer approximation, with the nuclear part described by the lattice dynamics. The ions in a crystalline solid move in a periodic pattern and vibrate around their equilibrium positions. Following the theory of lattice dynamics, the vibrational frequencies $\omega(\mathbf{q})$ are determined as the square root of the eigenvalues of the dynamical matrix $D_{sa,t\beta}(\mathbf{q})$:²⁹

$$D_{sa,t\beta}(\mathbf{q}) = \frac{1}{\sqrt{M_s M_t}} \sum_l \Phi_{ls\alpha,0t\beta} \exp[i\mathbf{q} \cdot (\mathbf{R}_0 + \boldsymbol{\tau}_t - \mathbf{R}_l - \boldsymbol{\tau}_s)], \quad (1)$$

which is the lattice Fourier transformation of the force constants exerted on the ions. Here, $\mathbf{R}_l + \boldsymbol{\tau}_s$ represents the equilibrium position of atom s with mass M_s in primitive cell l , and the sum runs over the infinite number of primitive cells in the crystal. $\Phi_{ls\alpha,0t\beta}$ is the force-constant matrix, given by the second-order derivatives of potential U with respect to the ionic displacement u_i , i.e., $\Phi_{ls\alpha,0t\beta} = \partial^2 U / \partial u_{i\alpha} \partial u_{0t\beta}$, evaluated with all atoms at their equilibrium positions, and α and β are Cartesian components.

However, this standard formulation does not include the nonanalytic term due to long-range interactions, which arise in polar systems because of the LRCI.^{1,2} A typical example is an ionic crystal, in which the relative displacement of charged cations and anions creates a macroscopic E-field that in turn affects the vibrations of the charged ions. These additional forces acting on ions are nonanalytic and can be expressed as a correction term to the dynamical matrix at small wave-vector \mathbf{q} near the ZC,²⁹

$$D_{sa,t\beta}^{na}(\mathbf{q} \rightarrow 0) = \frac{1}{\sqrt{M_s M_t}} \frac{4\pi e^2}{\Omega} \frac{(\mathbf{q} \cdot \mathbf{Z}_s^*)_\alpha (\mathbf{q} \cdot \mathbf{Z}_t^*)_\beta}{\mathbf{q} \cdot \boldsymbol{\epsilon}^\infty \cdot \mathbf{q}}, \quad (2)$$

where \mathbf{Z}_s^* is the Born effective charge tensor for atom s , $\boldsymbol{\epsilon}^\infty$ is the high-frequency static dielectric tensor, and Ω is the unit-cell volume. This nonanalytic correction lifts the energy degeneracy and induces LO-TO splitting around the Γ point in an ionic crystal.

Electrides are unique in that they are intrinsically polar even in their elemental phases, such as those of Li and Na.^{25–28} The spatial ion–electron separation and charge transfer in the system leads to dipole moments and the subsequent macroscopic E-field when the matrix atoms move around, very similar to the well-known case of ionic compounds. The fact that the highly localized excess electrons in an electrified form negatively charged ISQs, as well as the observations that ISQs remain almost intact when the matrix atoms vibrate under high-temperature/pressure conditions^{27,30} and that they could form

covalent bonds,^{31,32} give us confidence to map an electrified onto an ionic compound, with the matrix atoms and ISQs corresponding to the cations and anions, respectively. Also, this treatment strategy can be regarded as integrating the electronic degree of freedom to the sites and charge of the ISQs, which is a coarse-grained approach that is used widely in condensed-matter physics. This standard treatment of electrified makes it possible to describe the nonanalytic contribution of the LRCI in electrifieds by generalizing Eq. (2) to include ISQs as a new species. Therefore, the additional components for the nonanalytic dynamical matrix should be

$$D_{sa,(ISQ)\beta}^{na}(\mathbf{q} \rightarrow 0) = \frac{1}{\sqrt{M_s M_{ISQ}}} \frac{4\pi e^2}{\Omega} \frac{(\mathbf{q} \cdot \mathbf{Z}_s^*)_\alpha (\mathbf{q} \cdot \mathbf{Z}_{ISQ}^*)_\beta}{\mathbf{q} \cdot \boldsymbol{\epsilon}^\infty \cdot \mathbf{q}} \quad (3)$$

and

$$D_{(ISQ)'\alpha,(ISQ)''\beta}^{na}(\mathbf{q} \rightarrow 0) = \frac{1}{\sqrt{M_{(ISQ)'} M_{(ISQ)''}}} \times \frac{4\pi e^2}{\Omega} \frac{(\mathbf{q} \cdot \mathbf{Z}_{(ISQ)'}^*)_\alpha (\mathbf{q} \cdot \mathbf{Z}_{(ISQ)''}^*)_\beta}{\mathbf{q} \cdot \boldsymbol{\epsilon}^\infty \cdot \mathbf{q}}. \quad (4)$$

Equations (1)–(4) constitute the full dynamical matrix for an electrified.

In Eqs. (3) and (4), we introduce \mathbf{Z}^* for the anionic ISQs, which unfortunately cannot be evaluated directly by using current first-principles polarization theory. Nevertheless, they can be estimated with the help of lattice symmetry and the acoustic sum rule of $\sum_k \mathbf{Z}_{k,\alpha\beta}^* = 0$. Alternatively, because the Bader charge of the matrix atoms and ISQs can be readily computed using the electron density,³³ it is plausible to approximate \mathbf{Z}^* in Eqs. (2)–(4) by the Bader charge.³⁴ As for the relative atomic mass of the ISQs (M_{ISQ}), we take the approximation of $M_{ISQ} \rightarrow \infty$ following the observation that the positions of the ISQs in Li and Na remain almost unchanged during vibration of the matrix atoms. On the other hand, the change in the ISQs induced by the lattice atoms is similar to plasmon oscillation, and the motion frequency of a plasmon is $\omega = \sqrt{\frac{4\pi e^2 n_e}{m^*}}$, where m^* is the effective mass of the electrons. For electrifieds, the valence electrons are highly localized in the interstitial sites, so their effective mass m^* is very large, which leads to a relatively small excitation frequency and relatively slow collective motion. Therefore, the vibration of the ISQs in an electrified can be coupled with the matrix atoms. Nevertheless, the impact of M_{ISQ} on the phonon dispersion is discussed in the following sections by using a finite value.

B. Computational details

We explored how LRCI affects the phonon dispersion [Eqs. (2)–(4)] in promising electrifieds at various pressures, including Li, Na, K, Rb, Cs, Sr, Be, Mg, and Ca. Here, only the results for dense fcc-Li and hP4-Na (see Fig. 1) are reported. The structural relaxation and force calculation are carried out with density functional theory^{35,36} as implemented in the Vienna *Ab initio* Simulation Package (VASP).^{37–39} The projector-augmented wave pseudo-potential^{39,40} method and plane-wave basis set are employed. The Perdew–Burke–Ernzerhof generalized-gradient approximation is used for the electronic exchange-correlation functional.⁴¹ The $1s^2 2s^1$ and $2s^2 2p^6 3s^1$ electrons are included in the valence space for Li and Na, respectively. The required forces are computed using a $5 \times 5 \times 5$

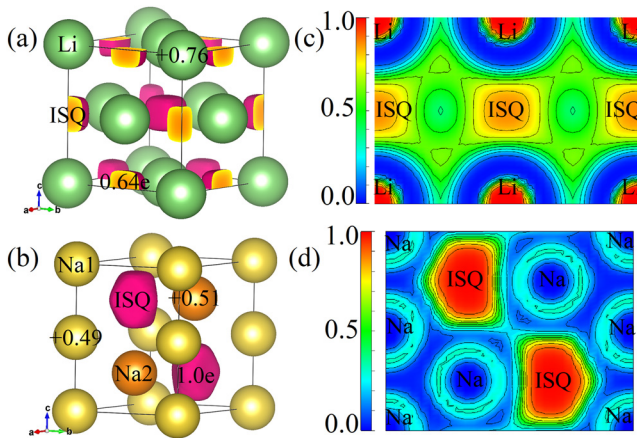


FIG. 1. Electron localization function (ELF) of (a) fcc-Li at 40 GPa and (b) hP4-Na at 300 GPa (isosurface = 0.75). The charge states of atoms and interstitial quasi-atoms (ISQs) are indicated. Note the prominent charge transfer and polarization. (c) and (d) show the ELF in the (1 1 0) plane of (a) and (b), respectively.

supercell containing 125 atoms with an energy cutoff of 1 keV in the fcc-Li phase and a $4 \times 4 \times 3$ supercell containing 192 atoms with an energy cutoff of 1 keV in the hP4-Na phase. Γ -centered k -point meshes of $5 \times 5 \times 5$ and $3 \times 3 \times 3$ are used to sample the Brillouin zone. The total energy is ensured to converge to within 1×10^{-6} eV/atom. All investigated structures are fully relaxed at the given pressure until the Hellmann–Feynman forces acting on all atoms are less than 0.001 eV/Å and the total stress tensor has converged to the hydrostatic state within 0.01 GPa. Z^* and ϵ^∞ are evaluated using the density functional perturbation theory method as proposed by Baroni and Resta⁴² and implemented in VASP. The Bader charge, as an alternative approximation to Z^* , is calculated using the Bader charge analysis code.^{43–45}

III. RESULTS

We begin by considering the limiting case of $M_{ISQ} \rightarrow \infty$, in which the anionic ISQs are frozen and unresponsive to the vibrations of the matrix atoms. Figures 2(a) and 2(b) show the calculated $\omega(\mathbf{q})$ relation for isotropic dense fcc-Li at 40 GPa in this limit. The results represent a paradigm shift from the common wisdom about elemental metals. It is well known that the fcc structure has only one atom in the primitive cell, and all such structures have only three acoustic branches, with no optical modes. Therefore, there can be no LO-TO splitting even when there is charge transfer from the matrix atoms to the lattice interstices. However, completely unexpectedly, we observe an energy splitting near the ZC (Γ point). Interestingly, this splitting occurs in the acoustic modes rather than the expected optical modes. In other words, the long-range interaction in the fcc-Li electride induces an anomalous LA-TA splitting that is analogous to the LO-TO splitting in ionic compounds. To understand this effect, note the introduction of localized electrons as a new species of ISQs to the electride lattice, which gives the original acoustic modes the characteristics of optical modes. In-depth analysis reveals that it is the direct participation of electrons in the lattice dynamics that leads to this acoustic branch splitting. We find that the two TA modes still have zero energy at the Γ point, but the LA mode gains nonzero energy and rises to a higher level at and near the Γ point. The frequency lift ($\Delta\omega = \omega_{LA} - \omega_{TA}$) ranges from 140 to 430 cm^{-1} according to whether the Born effective charge or the Bader charge is used. Note that the general features of the splitting are robust and independent of the approximations that were used.

The high-pressure phase of sodium (hP4-Na) is reported as a typical representative of the anisotropic case [see Figs. 2(c) and 2(d)]. Here, $\Delta\omega$ (25–132 cm^{-1}) is much smaller than that in fcc-Li. Note that the Bader charge of the ISQs in hP4-Na is $\sim 1.1e$, compared to $\sim 0.6e$ in fcc-Li. The reduction in $\Delta\omega$ is due mainly to the larger dielectric constant in the hP4-Na phase ($\epsilon_{xx}^\infty = \epsilon_{yy}^\infty = 5.8$, $\epsilon_{zz}^\infty = 13.1$). For comparison, this value is $\epsilon_{xx}^\infty = \epsilon_{yy}^\infty = \epsilon_{zz}^\infty = 1.6$ in fcc-Li. The structure of hP4-Na is unique because of the lattice anisotropy, which also

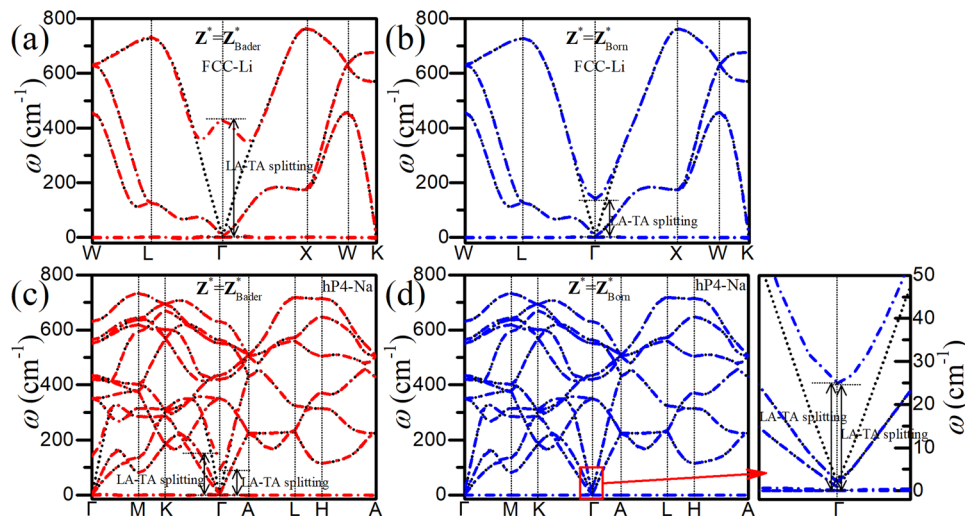


FIG. 2. Phonon dispersions of isotropic fcc-Li at 40 GPa [(a) and (b)] and anisotropic hP4-Na at 300 GPa [(c) and (d)] calculated using Bader charge [(a) and (c)] and Born effective charge [(b) and (d)] (dot-dash lines), which are compared with the bare results obtained without accounting for the LRCI contribution (dotted lines).

makes the LA-TA splitting anisotropic. As shown in Figs. 2(c) and 2(d), $\Delta\omega(\mathbf{q} \approx 0)|_{K \rightarrow \Gamma}$ is not equal to $\Delta\omega(\mathbf{q} \approx 0)|_{A \rightarrow \Gamma}$. Note that in Fig. 2(d), the nonanalytical LRCI is almost suppressed when compared to Fig. 2(c). This is because the modern theory of polarization cannot capture properly the electron localization in the lattice interstices and the resultant polarization, thereby underestimating the charge state of the matrix atoms. In this regard, the Bader charge (which is a scheme based on real space division) is better for describing the charge state and polarization in electrides. For example, in fcc-Li at 40 GPa, the charge state of the matrix atoms is $\sim 0.76e$ with the Bader charge compared to $\sim 0.20e$ with the Born effective charge, i.e., ~ 3.8 times larger. The difference between Born effective charge and Bader charge linearly scales down the $\Delta\omega$ in Fig. 2 (see Fig. S1 in the supplementary material).

The influence of ϵ^∞ is explored by artificially changing its value to investigate how the $\omega(\mathbf{q})$ curve is impacted. As shown in Fig. 3(a), when ϵ^∞ of hP4-Na is intentionally modified from $\epsilon_{xx}^\infty = \epsilon_{yy}^\infty = 5.8, \epsilon_{zz}^\infty = 13.1$ to $\epsilon_{xx}^\infty = \epsilon_{yy}^\infty = \epsilon_{zz}^\infty = 5.8$, $\Delta\omega(\mathbf{q} \approx 0)|_{K \rightarrow \Gamma}$ becomes equal to $\Delta\omega(\mathbf{q} \approx 0)|_{A \rightarrow \Gamma}$, and the LA-TA splitting becomes isotropic. On the other hand, $\Delta\omega$ for both fcc-Li and hP4-Na decreases sharply with increasing dielectric constant, and $\Delta\omega$ approaches a small constant for $\epsilon^\infty > 10$ [see Fig. 3(b)]. This shows not only that the magnitude of LA-TA splitting is inversely proportional to the square root of ϵ^∞ , as indicated by Eq. (2), but also that ϵ^∞ is an important source of the anisotropy. Note that \mathbf{Z}^* also contains anisotropy information, which however is missed if the Bader charge is used.

To gain insight into the effect of the dynamic ISQ response, we lift the constraint of $M_{\text{ISQ}} \rightarrow \infty$. Figures 4(a) and 4(b) (see Figs. S2–S4

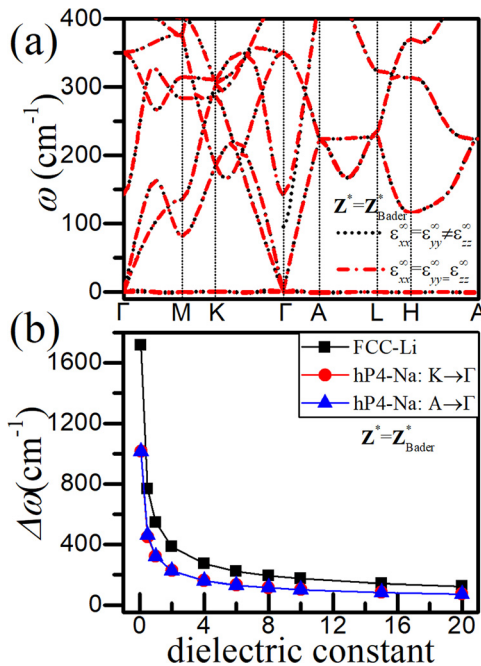


FIG. 3. (a) Phonon dispersion of hP4-Na at 300 GPa calculated with artificially varied ϵ^∞ . (b) Variations of $\Delta\omega = \omega_{\text{LA}} - \omega_{\text{TA}}$ with ϵ^∞ in fcc-Li at 40 GPa and hP4-Na at 300 GPa.

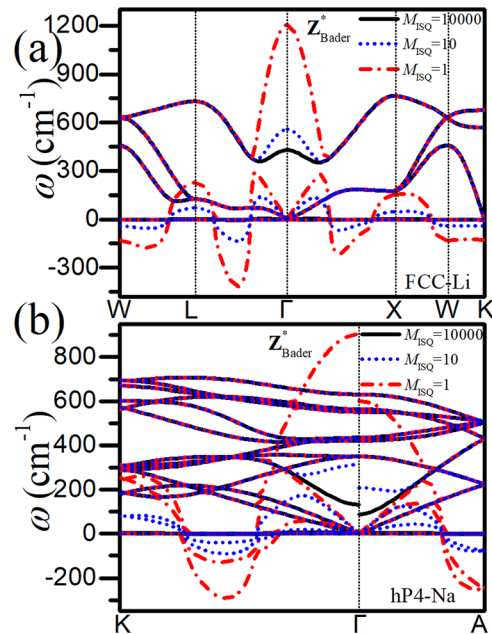


FIG. 4. Phonon dispersions of (a) fcc-Li at 40 GPa and (b) hP4-Na at 300 GPa calculated with different values of effective mass M_{ISQ} .

in the supplementary material) show how the $\omega(\mathbf{q})$ curves of fcc-Li and hP4-Na, respectively, vary when M_{ISQ} changed from 10 000 to 1. It is evident that the movable ISQs provide an additional mode that takes the place of the original LA branch, whereas the original LA mode moves up to become a special “optical mode” that has relative displacements against the anionic ISQs. There are two band-crossing avoidances near the ZC, suggesting that both the moved-up “optical mode” and the left-behind LA mode have mixed contributions from both matrix atoms and ISQs. The fluctuating LA mode with small M_{ISQ} implies strong energy dissipation by electrons when an acoustic wave propagates through the electride. Nevertheless, because electrons have strong quantum characteristics, this classical mode of the ISQs might be invalid when M_{ISQ} is small. The important insight gained from this analysis is that the fictitious LA mode of electrons can be suppressed if the ISQs are irresponsive to the lattice vibrations, and in this case the resultant LA-TA splitting has explicit physical implications. The uplifted LA mode contains significant contributions from electrons, i.e., it is the energy from the strong electron-phonon coupling that lifts the LA-TA degeneracy. Also shown is that if the ISQs become responsive, then the strong electron-phonon coupling breaks the current standard theory of lattice dynamics, and electrides must be treated with both electrons and matrix atoms on the same footing.

IV. DISCUSSION

By a thorough and comprehensive study of dense Li and Na, as well as many other promising electrides not reported here, we arrive at criteria (or rules of thumb) for the LA-TA splitting in an electride to occur: (i) the Bader charge of the ISQs must be greater than $0.2e$ and (ii) ϵ^∞ must not exceed 10, otherwise the LA-TA splitting could be too small to be observed.

We also noticed that to have strong anisotropic LA-TA splitting, the electricle should have very strong anisotropy in the dielectric tensor, or strong anisotropy in Z^* . Note that the dynamic response of the ISQs to lattice vibration has a strong impact on the phonon dispersion. If $M_{\text{ISQ}} \rightarrow \infty$ is valid, then the LA-TA splitting is governed by Eq. (2), which can be applied to zero-, one-, and two-dimensional electriles. For finite M_{ISQ} , the counterparts to Eqs. (3) and (4) for one- and two-dimensional electriles can be derived straightforwardly following similar reasoning; however, that is beyond the present scope and is not elaborated here.

The nonanalytic correction for the LRCI of Eqs. (2)–(4) is applicable as long as no zero polarization is generated during the lattice vibrations. In an electricle, this term becomes null only when the ISQs respond to the movement of the matrix atoms in a special manner such that all the involved atom–ISQ distances scale linearly to cancel the generated dipoles. This subtle geometric balance is very rare, if not totally impossible. Such scaling correlation maintains the local relative positions of the ISQs with respect to the matrix atoms, thus no LRCI occurs. We did not observe this type of correlation in dense fcc-Li, but if it were to arise, this subtle balance could be removed by imposing an external magnetic or electric field.

V. CONCLUSION

A theory was proposed for modeling the nonanalytic contribution to the lattice phonons of the LRCI that should be present in an electricle. An anomalous LA-TA splitting was predicted in dense fcc-Li and hP4-Na, and the direct effects of the participation of localized electrons in lattice vibrational propagation as anionic ISQs were discovered. The strong electron (ISQ)–phonon coupling was revealed. After a thorough and extensive investigation of promising candidates for electriles, criteria (or rules of thumb) for observable LA-TA splitting were summarized, which provide guidelines for experimentalists to design an appropriate experiment to detect this unconventional LA-TA splitting phenomenon. We also concluded that when electrons and ISQs are highly responsive to the lattice motion, then the classical theory of lattice dynamics breaks down, and the electrons and matrix atoms must be treated on the same footing with full quantum mechanics for this type of mobile electricle. In practical applications, crystal defects, especially the potential colossal-charge-state impurities in electriles,⁴⁶ may have striking influence on the local vibrational and optical properties of this class of emerging materials.

SUPPLEMENTARY MATERIAL

See the [supplementary material](#) for information about the variation of $\Delta\omega$ with different Bader charge values and different M_{ISQ} .

ACKNOWLEDGMENTS

This work was supported by the National Natural Science Foundation of China (Grant No. 11672274), the National Natural Science Foundation of China and the China Academy of Engineering Physics (NSAF) (Grant No. U1730248), the Science Challenge Project (Grant No. TZ2016001), and the China Academy of Engineering Physics Research Project No. CX2019002.

DATA AVAILABILITY

The data that support the findings of this study are available within the article and its [supplementary material](#).

REFERENCES

- 1 M. Born and K. Huang, *Dynamical Theory of Crystal Lattices* (Oxford University Press, 1954).
- 2 N. W. Ashcroft and N. D. Mermin, *Solid State Physics* (Dryden Press, 1976).
- 3 S. S. Mitra, “Grüneisen parameter for long wavelength optical modes in ionic crystals,” *Phys. Status Solidi* **9**(2), 519 (1965).
- 4 A. S. Barker and H. W. Verleur, “Long wavelength optical phonon vibrations in mixed crystals,” *Solid State Commun.* **5**(9), 695 (1967).
- 5 S. S. Mitra, C. Postmus, and J. R. Ferraro, “Pressure dependence of long-wavelength optical phonons in ionic crystals,” *Phys. Rev. Lett.* **18**(12), 455 (1967).
- 6 M. C. Abramo, M. Parrinello, M. P. Tosi, and D. E. Thornton, “Optical modes in binary alloys,” *Phys. Lett. A* **43**(6), 483 (1973).
- 7 R. J. Crook, F. Yang, and J. R. Sambles, “Long-range optical modes supported by a strongly absorbing thin organic film,” *J. Opt. Soc. Am. B* **10**(2), 237 (1993).
- 8 G. Komandin, O. Porodinkov, I. Spektor, S. Chuchupal, and A. Volkov, “Giant LO-TO frequency splitting of the soft mode in perovskites,” *Ferroelectrics* **463**(1), 1 (2014).
- 9 J. S. Landers, J. L. Dye, A. Stacy, and M. J. Sienko, “Temperature-dependent electron spin interactions in lithium [2.1.1] cryptate electricle powders and films,” *J. Phys. Chem.* **85**(9), 1096 (1981).
- 10 S. Matsui, Y. Toda, M. Miyakawa, K. Hayashi, T. Kamiya, M. Hirano, I. Tanaka, and H. Hosono, “High-density electron anions in a nanoporous single crystal: $[\text{Ca}_{24}\text{Al}_{28}\text{O}_{64}]^{4+}(4e^-)$,” *Science* **301**(5633), 626 (2003).
- 11 M.-S. Miao and R. Hoffmann, “High pressure electriles: A predictive chemical and physical theory,” *Acc. Chem. Res.* **47**(4), 1311 (2014).
- 12 Y. Zhang, H. Wang, Y. Wang, L. Zhang, and Y. Ma, “Computer-assisted inverse design of inorganic electriles,” *Phys. Rev. X* **7**(1), 011017 (2017).
- 13 L. A. Burton, F. Ricci, W. Chen, G.-M. Rignanese, and G. Hautier, “High-throughput identification of electriles from all known inorganic materials,” *Chem. Mater.* **30**(21), 7521 (2018).
- 14 Q. Zhu, T. Frolov, and K. Choudhary, “Computational discovery of inorganic electriles from an automated screening,” *Matter* **1**(5), 1293 (2019).
- 15 P. Li, G. Gao, Y. Wang, and Y. Ma, “Crystal structures and exotic behavior of magnesium under pressure,” *J. Phys. Chem. C* **114**(49), 021745 (2010).
- 16 C. J. Pickard and R. J. Needs, “Aluminium at terapascal pressures,” *Nat. Mater.* **9**(8), 624 (2010).
- 17 M. Martínez-Canales, C. J. Pickard, and R. J. Needs, “Thermodynamically stable phases of carbon at multiterapascal pressures,” *Phys. Rev. Lett.* **108**(4), 045704 (2012).
- 18 Y.-M. Chen, H.-Y. Geng, X.-Z. Yan, Z.-W. Wang, X.-R. Chen, and Q. Wu, “Predicted novel insulating electricle compound between alkali metals lithium and sodium under high pressure,” *Chin. Phys. B* **26**(5), 056102 (2017).
- 19 J. Zhou, L. Shen, M. Yang, H. Cheng, W. Kong, and Y. P. Feng, “Discovery of hidden classes of layered electriles by extensive high-throughput material screening,” *Chem. Mater.* **31**(6), 1860 (2019).
- 20 B. Wan, J. Zhang, L. Wu, and H. Gou, “High-pressure electriles: From design to synthesis,” *Chin. Phys. B* **28**(10), 106201 (2019).
- 21 J. L. Dye, “Electriles: Ionic salts with electrons as the anions,” *Science* **247**(4943), 663 (1990).
- 22 D. J. Singh, H. Krakauer, C. Haas, and W. E. Pickett, “Theoretical determination that electrons act as anions in the electricle $\text{Cs}^+(15\text{-crown-5})_2\text{-e}^-$,” *Nature* **365**(6441), 39 (1993).
- 23 J. L. Dye, “Electrons as anions,” *Science* **301**(5633), 607 (2003).
- 24 X. Zhang and G. Yang, “Recent advances and applications of inorganic electriles,” *J. Phys. Chem. Lett.* **11**(10), 3841 (2020).
- 25 J. B. Neaton and N. W. Ashcroft, “Pairing in dense lithium,” *Nature* **400**(6740), 141 (1999).

- ²⁶M. Marqués, M. I. McMahon, E. Gregoryanz, M. Hanfland, C. L. Guillaume, C. J. Pickard, G. J. Ackland, and R. J. Nelmes, "Crystal structures of dense lithium: A metal-semiconductor-metal transition," *Phys. Rev. Lett.* **106**(9), 095502 (2011).
- ²⁷Y. Ma, M. Eremets, A. R. Oganov, Y. Xie, I. Trojan, S. Medvedev, A. O. Lyakhov, M. Valle, and V. Prakapenka, "Transparent dense sodium," *Nature* **458**(7235), 182 (2009).
- ²⁸Z. Yu, H. Y. Geng, Y. Sun, and Y. Chen, "Optical properties of dense lithium in electride phases by first-principles calculations," *Sci. Rep.* **8**(1), 3868 (2018).
- ²⁹D. Alfè, "PHON: A program to calculate phonons using the small displacement method," *Comput. Phys. Commun.* **180**(12), 2622 (2009).
- ³⁰R. Paul, S. X. Hu, V. V. Karasiev, S. A. Bonev, and D. N. Polsin, "Thermal effects on the electronic properties of sodium electride under high pressures," *Phys. Rev. B* **102**, 094103 (2020).
- ³¹M.-s. Miao and R. Hoffmann, "High-pressure electrides: The chemical nature of interstitial quasiatoms," *J. Am. Chem. Soc.* **137**(10), 3631 (2015).
- ³²M.-s. Miao, R. Hoffmann, J. Botana, I. I. Naumov, and R. J. Hemley, "Quasi-molecules in compressed lithium," *Angew. Chem., Int. Ed.* **56**(4), 972 (2016).
- ³³R. F. W. Bader, "Atoms in molecules: A quantum theory," *J. Mol. Struct.: THEOCHEM* **360**, 1 (1996).
- ³⁴W. Tang, E. Sanville, and G. Henkelman, "A grid-based Bader analysis algorithm without lattice bias," *J. Phys.: Condens. Matter* **21**(8), 084204 (2009).
- ³⁵P. Hohenberg and W. Kohn, "Inhomogeneous electron gas," *Phys. Rev.* **136**(3B), B864 (1964).
- ³⁶W. Kohn and L. J. Sham, "Quantum density oscillations in an inhomogeneous electron gas," *Phys. Rev.* **137**(6A), A1697 (1965).
- ³⁷G. Kresse and J. Furthmüller, "Efficient iterative schemes for ab initio total-energy calculations using a plane-wave basis set," *Phys. Rev. B* **54**, 011169 (1996).
- ³⁸G. Kresse and J. Furthmüller, "Efficiency of ab-initio total energy calculations for metals and semiconductors using a plane-wave basis set," *Comput. Mater. Sci.* **6**(1), 15 (1996).
- ³⁹G. Kresse and D. Joubert, "From ultrasoft pseudopotentials to the projector augmented-wave method," *Phys. Rev. B* **59**(3), 1758 (1999).
- ⁴⁰P. E. Blöchl, "Projector augmented-wave method," *Phys. Rev. B* **50**, 017953 (1994).
- ⁴¹J. P. Perdew, K. Burke, and M. Ernzerhof, "Generalized gradient approximation made simple," *Phys. Rev. Lett.* **77**, 3865 (1996).
- ⁴²S. Baroni and R. Resta, "Ab initio calculation of the macroscopic dielectric constant in silicon," *Phys. Rev. B* **33**(10), 7017 (1986).
- ⁴³E. Sanville, S. D. Kenny, R. Smith, and G. Henkelman, "An improved grid-based algorithm for Bader charge allocation," *J. Comput. Chem.* **28**(5), 899 (2007).
- ⁴⁴G. Henkelman, A. Arnaldsson, and H. Jónsson, "A fast and robust algorithm for Bader decomposition of charge density," *Comput. Mater. Sci.* **36**(3), 354 (2006).
- ⁴⁵M. Yu and D. R. Trinkle, "Accurate and efficient algorithm for Bader charge integration," *J. Chem. Phys.* **134**, 064111 (2011).
- ⁴⁶L. Zhang, Q. Wu, S. Li, Y. Sun, X. Yan, Y. Chen, and H. Y. Geng, "Interplay of anionic quasi-atoms and interstitial point defects in electrides: Abnormal interstice occupation and colossal charge state of point defects in dense fcc-lithium," *ACS Appl. Mater. Interfaces* **13**(5), 6130 (2021).